# 1 F1306: Adaptive Multilevel Methods for Nonlinear 3D Mechanical Problems

*Title :* Adaptive Multilevel Methods for Nonlinear 3D Mechanical Problems

*Principal investigator :* Prof. Dr. Ulrich Langer
Institute of Computational Mathematics
Johannes Kepler University Linz
Phone: +43-70-2468-9168
Fax: +43-70-2468-9148
E-Mail: ulanger@numa.uni-linz.ac.at

*Co-investigator :* Prof. Dr. Joachim Schöberl
MATHCCES - Department for Mathematics CCES
RWTH Aachen University, Germany
Phone: +49-241-963-2133
E-Mail: joachim.schoeberl@rwth-aachen.de

Disciplinary affiliation:

| 1 | % | 2 | % | 3 | % |
|---|---|---|---|---|---|
| 1114 | 35 | 2541 | 35 | 1140 | 30 |

(according to the Central Bureau of Statistics classification)

## 1.1 Abstract

In the first funding period, this subproject was concerned with magneto-mechanical problems. During the first year of the second funding period, we have finished this research work on magneto-mechanical problems that was based on a direct cooperation of mathematicians (Langer's group) and engineers (Lerch's group) in one project.

During the second funding period we have investigated and implemented two new classes of problems: 3D elasto-plastic flow problems and piezo-electrical problems. Both problems are coupled field problems, but in a different sense. *Piezo-electrical problems* are coupled field problems in which the electrical field interacts with the mechanical field in the whole computational domain. whereas in *elastoplasticity* we have to deal with an unknown and time evolving elastoplastic interface, which separates the computational domain into parts. This elasto-plastic deformation process can be modeled by some time-dependent quasi-variational inequality that results in a sequence of variational inequalities with a non-differential term after time discretization.

The third period is entirely dedicated to the investigation of elastoplastic problems.

In particular we have studied two very different solution algorithms, as described in the subsections 1.3.1 and 1.3.2, and we applied nested iteration techniques (cf. the subsections 1.3.3 and 1.3.4) in order to speed up the solution algorithms. Moreover, we investigated more complicated models of elastoplasticity as well as proper a posteriori error estimates and finite elements for standard models (see the subsections 1.3.5 and 1.3.6). The former postdoc Dr. J. Schöberl accepted a professorship at the RWTH Aachen and remained as the project co-investigator.

This report is only concerned with the documentation on the third funding period. Let us begin with summarizing the substantial contributions (publications and software) to the goals of this subproject, which can be seen in the Table below:

| Attained Goals | References |
|---|---|
| **Elasto-Plastic Materials** | [8], [5], [6], [7], [17], [20], [29], [28], [31], [33], [32], [10], [11], [24], [25] |
| Other Mechanical Applications | [43], [41] |
| **Master's theses** | [18], [40] |
| **Ph.D. theses** | [30] |
| **Software** | |
| `Packages for NGSolve` | www.sfb013.uni-linz.ac.at/software.html |

In summary, we published 5 papers in refereed journals, 4 papers in refereed proceedings, 1 paper in proceedings, and 7 technical reports. In addition, 1 Ph.D. theses and 2 Master's theses were completed during the third funding period.

## 1.2 Scientific Background and Current State of Research

Elasto-plastic material behavior is often exploited in many engineering problems for calculation of permanent deformation of structures, stability in the structural and solid mechanics and other processes beyond elasticity. Mathematical and numerical aspects of problems in elasto-plasticity date back to works of Duvaut and Lions [15], Johnson [27], and Korneev and Langer [34]. More recent works on this topic can be found in Hlaváček et al. [23], Johnson et al. [16], Han and Reddy [21, 22], Simo and Hughes [26], Stein et al. [46], amongst others.

A typical problem is a mechanical object fixed on some part of the boundary (Dirichlet boundary conditions), which is subjected to surface traction on some other parts of the boundary. The screw wrench from Schwarz [45] in Figure 1(a) belongs to this problem class. It is fixed by an immobile screw, which results in homogenous Dirichlet boundary conditions. The forces acting on the handle are assumed to be acting in the vertical direction only. The result is given in Figure 1(b), where the blue zone is the elastic one and the red areas are the the plastic ones, where permanent deformation has occurred.

For demonstrating the striking difference between purely elastic and elastoplastic calculations, the von-Mises stress for the screw wrench is compared: In Figure 2(a) the

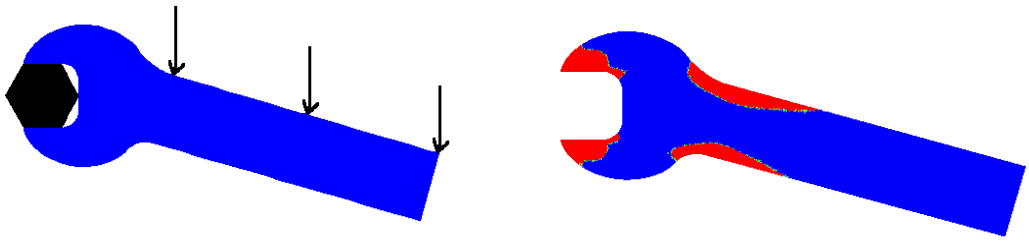

(a) (b)

Figure 1: (a) Screw wrench; (b) plasticity domain

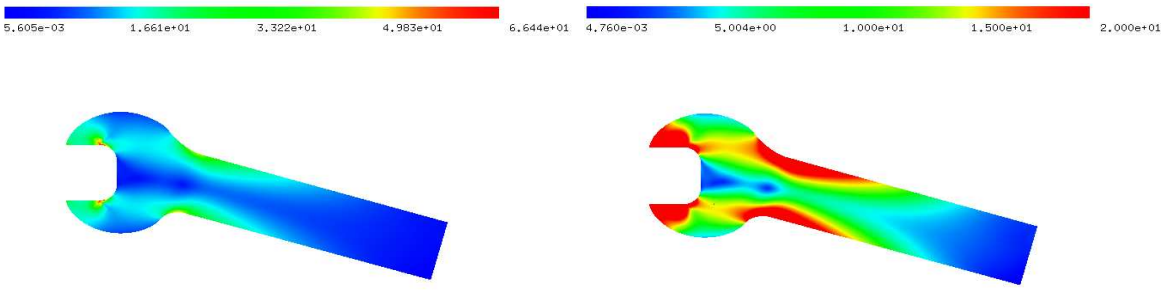


(a) (b)

Figure 2: (a) The von-Mises stress for the purely elastic wrench (values from 0 to $66\frac{\mathrm{N}}{\mathrm{mm}^2}$); (b) the von-Mises stress in plasticity (values from 0 to $20\frac{\mathrm{N}}{\mathrm{mm}^2}$)

stress varies from approximately zero up to $66\frac{\mathrm{N}}{\mathrm{mm}^2}$. For the elastoplastic screw wrench in Figure 2(b) the von-Mises stress can only attain a certain maximal value, which is here chosen as $20\frac{\mathrm{N}}{\mathrm{mm}^2}$. If this threshold is exceeded, the material undergoes permanent deformation and the plastic zones as in Figure 1(b) are obtained.

Elasto-plastic materials are described by six governing equations, see e.g. Carstensen [9]: According to the basic theorem of Cauchy, the stress field has to fulfill the equations

$$\sigma = \sigma^T \quad \text{in } \Omega, \tag{1}$$

$$-\operatorname{div} \sigma = b \quad \text{in } \Omega, \tag{2}$$

with $b$ being the vector field of given body forces. The linearized Cauchy-Green strain tensor is appropriate in the case of small deformations, and is given by

$$\varepsilon(u) = \frac{1}{2}(\nabla u + (\nabla u)^T)\,. \tag{3}$$

Moreover, in the case of small deformations the strain is split additively into two parts:

$$\varepsilon(u) = \mathbb{A}\,\sigma + p \quad \text{a. e. in } \Omega. \tag{4}$$

Here, $\mathbb{A}\,\sigma$ denotes the elastic, and $p$ the plastic strain. Purely elastic material behavior is characterized by $p \equiv 0$. The modeling of plasticity requires another material law in order to determine $p$. There are restrictions on the stress variables described by a dissipation functional $\varphi$, which is convex, and non-negative, but may also attain $+\infty$. The first restriction is

$$\varphi(\sigma, \alpha) < \infty \quad \text{a. e. in } \Omega. \tag{5}$$

The internal hardening parameter $\alpha$ is the memory of the considered body and describes previous plastic deformations. Its structure and dimension depend on the hardening law. The above inequality indicates that $\alpha$ controls the set of admissible stresses. The pair $(\sigma, \alpha)$ is called generalized stresses and values are called admissible if $\varphi(\sigma, \alpha) < \infty$. The time development of $p$ and $\alpha$ is given by the Prandtl-Reuß normality law which states that for all other generalized stresses $(\tau, \beta)$ there holds:

$$\dot{p} : (\tau - \sigma) - \dot{\alpha} : (\beta - \alpha) \leq \varphi(\tau, \beta) - \varphi(\sigma, \alpha) \quad \text{a. e. in } \Omega, \tag{6}$$

where $\dot{p}$ denotes the time derivative of $p$, i.e., $\dot{p} = \frac{\partial p}{\partial t}$, and $:$ is the scalar product of matrices such that $A : B = \sum_{i,j=1}^{n} A_{ij} B_{ij}$ for all $A, B \in \mathbb{R}^{n \times n}$. The relations (1)-(6) are equivalent to a variational problem with one equality in the stress and the strain, and one time-dependent inequality resulting from the normality law. This problem is solved by an implicit time discretization, e.g. an implicit Euler scheme.

The variational problem in each time step can be reformulated as an optimization problem still depending on the hardening law. In the case of isotropic hardening (see Alberty, Carstensen and Zarrabi [1]) it reads as a minimization problem in the displacement $u$ and the plastic strain $p$:

$$\begin{aligned} f(u,p) := \frac{1}{2} \int_\Omega \mathbb{C}\,[\varepsilon(u) - p] : (\varepsilon(u) - p)\, dx + \frac{1}{2} \int_\Omega (\alpha_0 + \sigma_y H |p - p_0|)^2\, dx \\ + \int_\Omega \sigma_y\, |p - p_0|\, dx - \int_\Omega b\, u\, dx \to \min \end{aligned} \tag{7}$$

under the constraint $\operatorname{tr}|p - p_0| = 0$, where $\alpha_0$ and $p_0$ are the variables from the previous time step and $\mathbb{C} = \mathbb{A}^{-1}$ is the elasticity matrix. The minimization problem is discretized by the use of the finite element method. This results in a finite dimensional minimization problem of the same form as above. It is known that the second variable $p$ depends on the first variable $u$ (see Alberty, Carstensen and Zarrabi [1]) such that for a given $u$ an optimal $p_{opt}(u)$ can be determined. Then, $f$ is minimized for a fixed $u$. The optimization problem thus reduces to one in a single variable

$$\min_u f(u, p_{opt}(u)). \tag{8}$$

The functional $f$ is continuous and convex, but not differentiable in the second variable $p$ on the whole domain. It is smooth in the purely elastic areas as well as in the purely plastic areas of the body considered. Across the interface it is only continuous, but not differentiable, since here the plastic variable $p$ changes its value from zero in the elastic case to a non-zero value for plasticity in a non-smooth manner.

## 1.3 Results and Discussion

The following two sections are concerned with the application of each a smoothing and a semismooth method to the optimization problem of elastoplasticity.

### 1.3.1 Solution Algorithm 1: Regularization of the energy functional

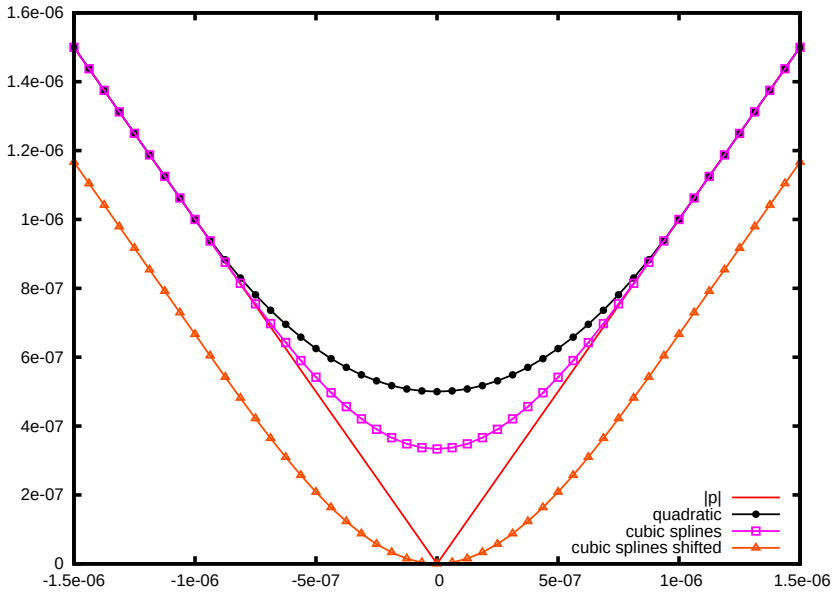


Figure 3: $|p|$ and its regularizations.

The first approach is to regularize $f$ and making it globally differentiable. This can be interpreted as reduction to a smooth functional in the displacements and the plastic strains. Figure 3 shows the modulus $|p|$ and possible regularizations $|p|_\epsilon$ depending on the regularization parameter $\epsilon$, $\epsilon$ is here chosen as $10^{-6}$. The green quadratic regularization within the interval $(-\epsilon, \epsilon)$ has a smooth first derivative, but the second derivative is piecewise constant and discontinuous, thus the local convergence of Newton type methods cannot be guaranteed. The blue piecewise cubic spline has a piecewise linear continuous second derivative, thus Newton type methods can be applied. The final choice is the pink regularization, where the blue cubic spline function is shifted into the origin, so that $|p|_\epsilon = 0$ holds for $p = 0$.

The necessary condition for the minimizer is that the Jacobian of $f$ is equal to zero. The system is transformed to a Schur-Complement only in the displacements. This system is then solved by an inexact Newton method, where the inverse is approximated by a multigrid preconditioned conjugate gradient method. The minimization with respect to the plastic strains is separable and several solution methods are given. Even an analytical solution $p(u)$ of the nonlinear minimization problem solely with respect to the plastic strains can be calculated. A linearized iteration scheme was constructed to overcome possible bad initial guesses, but it also performs well as self-contained solver. A Lax-Milgram analog based on the Banach fixed point theorem for nonlinear operators guarantees at least linear order of convergence. The developed algorithms are implemented in the finite element code NGSolve [37] of our group at the SFB. NGSolve stands here for both "New Generation Solver" and "NETGEN Solver", where NETGEN [36] is the automatic 3d tetrahedral mesh generator mainly developed by Schöberl [44].

The algorithms are extended towards uniform p-adaptivity, where p denotes the polynomial degree of the ansatz functions for the finite element spaces of $u$ and $p$. Düster [14] is one of the first to use high order finite elements for three-dimensional, thin-walled nonlinear continua. The first results on uniform p-refinement of our group are summarized in Kienesberger and Valdman [32]. In Nübel, Düster and Rank [39] and Nübel [38] the p-refinement is combined with a p-adaptive strategy on the interface, i.e. moving or removing nodes in the neighborhood such that the interface is approximated by the grid. For such a p-adaptive method exponential convergence can be expected.

The first version of the solvers worked only for linear displacements and piecewise constant plastic strains. Now the elastoplastic solver can handle higher polynomial ansatz functions for the finite element spaces of $u$ and $p$. These high order polynomials are investigated and implemented by the Start project group "Y-192" of Joachim Schöberl.

The considered test geometry is the two-dimensional plate fixed on the left edge and under traction in normal direction on the right edge. Figure 4 shows the yield function approximated by polynomials of degree 0, 2, 4, and 10 for several grids with uniformly refined mesh. According to theory and other numerical experiments, the p-method yields good approximation results for smooth functions.

If the solution is singular (e.g. in corners, for changing boundary conditions, or across the elastoplastic interface), the approximation property fails and can only be restored using h- or combined hp-methods. A global linear convergence result can be shown for such smoothing methods due to a Lax-Milgram analog which is based on the Banach fixed point theorem for nonlinear operators.

All details can be found in the PhD thesis of Johanna Kienesberger [30].

### 1.3.2 Solution Algorithm 2: Theorem of Moreau & Slanting Functions

Thanks to a theorem of Moreau [35] *(Prop. 7.d)* one can show, that the functional

$$F(v) := \inf_q f(v, q)$$

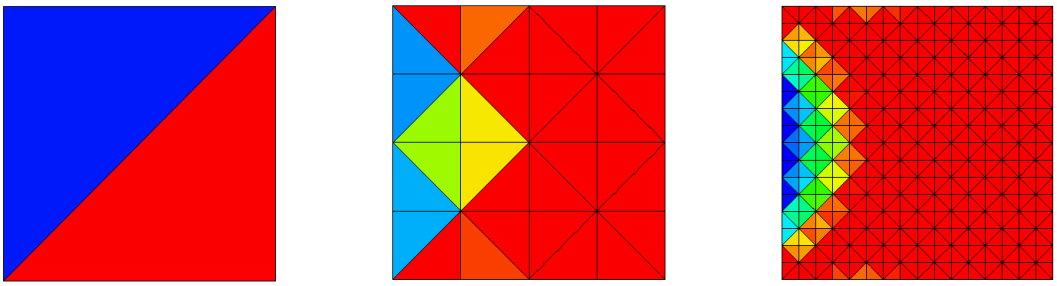

(a) $p = 0$, $h = 1$ (b) $p = 0$, $h = 1/4$ (c) $p = 0$, $h = 1/16$

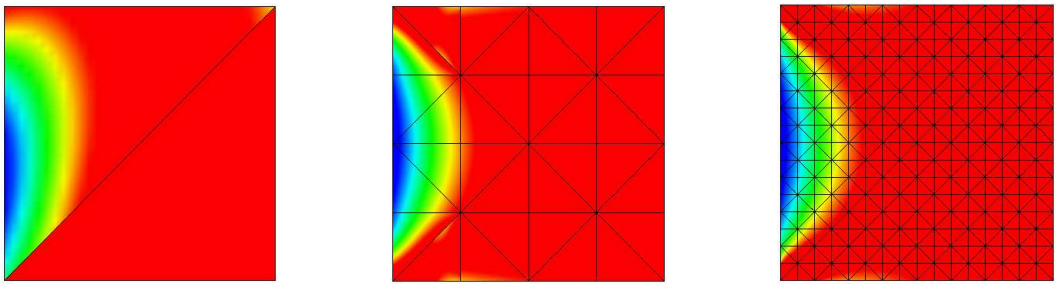

(d) $p = 2$, $h = 1$ (e) $p = 2$, $h = 1/4$ (f) $p = 2$, $h = 1/16$

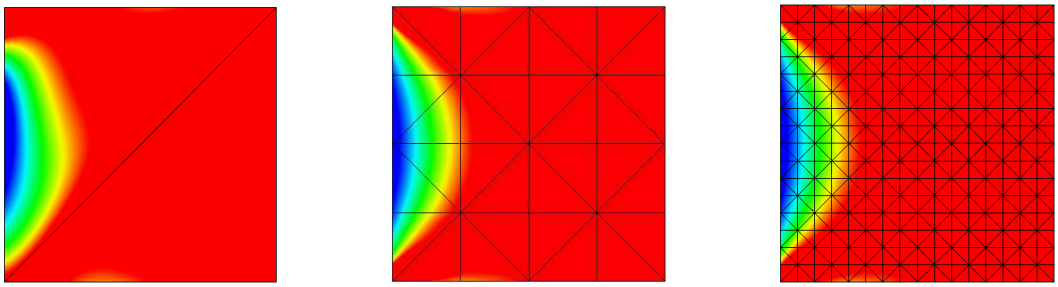

(g) $p = 4$, $h = 1$ (h) $p = 4$, $h = 1/4$ (i) $p = 4$, $h = 1/16$

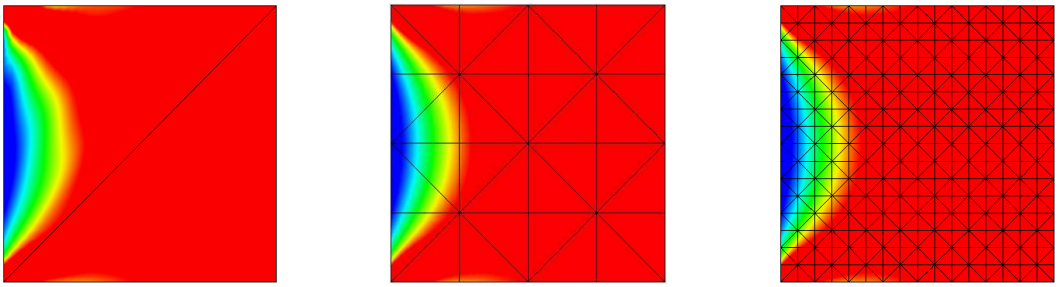

(j) $p = 10$, $h = 1$ (k) $p = 10$, $h = 1/4$ (l) $p = 10$, $h = 1/16$

Figure 4: First experiments for 2D elastoplasticity with uniform p-refinement

with $f$ defined in (7) is strictly convex and Fréchet differentiable, where the derivative of $F$ is explicitly computable, i. e., the Gâteaux differential into the direction $w$ reads

$$\mathrm{D}\, F(v;\, w) = \int_\Omega \mathbb{C}\,[\varepsilon(v) - p(\varepsilon(v))] : \varepsilon(w)\, \mathrm{d}x - \int_\Omega b^T w\, \mathrm{d}x\,.$$

Here the mapping $p(\varepsilon(v))$ denotes the plastic strain minimizer, which for all $v$ satisfies

$$F(v) = f(v, p(\varepsilon(v)))\,.$$

By using results of Alberty, Carstensen, and Zarrabi [1], who found the explicit form of $p(\varepsilon(v))$, the elastoplastic problem can now be solved by finding the displacement field $u$ such that the first derivative of $F$ vanishes. In this sense, a regularization of the former objective $f$ is no longer necessary. But unfortunately, $F$ is not twice differentiable, such that a classical Newton-Raphson scheme cannot be applied. However, a Newton-like method implemented in Matlab showed a super-linear convergence rate, cf. Table 1. Some numerical examples, as shown in Figure 5 and Figure 6, are outlined in the diploma thesis of Gruber [18], and the essential lines of code are presented in a technical report by Gruber and Valdman [17].

For a theoretical study of the observed super-linear convergence rate, so called *slanting functions* of the first derivative of $F$ turned out to be a convenient replacement for the lacking second derivative. The concept of slanting functions was recently introduced by Chen, Nashed, and Qi [13] and represents a massive tool for the development of semismooth methods, such as a slant Newton method which is of great use for our purpose. The research on the application of a slant Newton method on elastoplastic problems with hardening resulted in the following:

- In finite dimensions (after FE-discretization) the method converges locally super-linear.
- In infinite dimensions (without any spatial discretization) the method converges locally super-linear too, if an additional regularity condition is satisfied.

The validity of such regularity condition for general problems in elastoplasticity is still an open question. All the rigorous analysis to this topic can be found in a technical report of Gruber and Valdman [20], and are submitted for a journal publication.

Global linear convergence can be guaranteed for a slant Newton method with line search similarly to smoothing methods in Section 1.3.1. However, the quality of a slant Newton method obviously depends on two factors intrinsically:

- The efficient solution of the linear systems arising at each Newton step.
- The decrease of Newton steps, achieved by the prediction of proper initial values.

The first issue is studied in the context of the ongoing PhD thesis of P. G. Gruber, whereas the second is treated in the Master thesis of B. Rauchenschwandtner [40] (cf. Section 1.3.4).

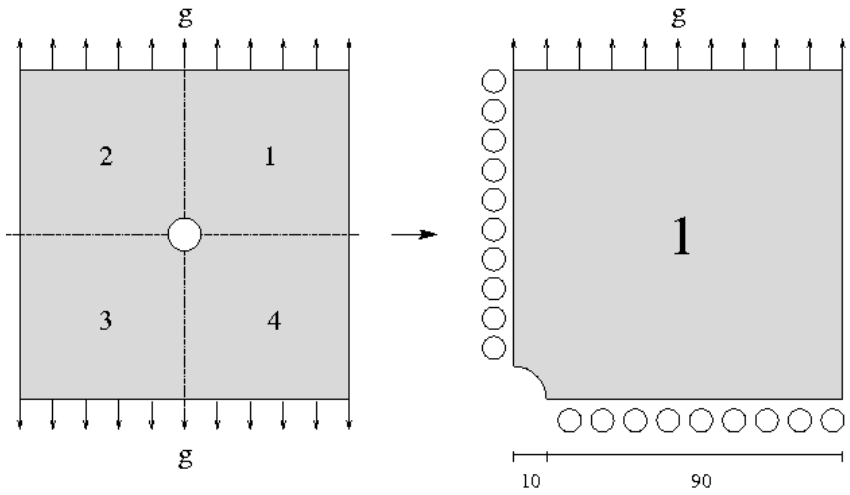


Figure 5: The example domain is a thin plate with a circular hole in the middle. A surface load $g$ is applied to the plate's upper and lower edge into normal direction. Just a single time step is considered, thus the surface load with the intensity $|g| = 450$ is acting instantly. Due to symmetry, the solution has to be calculated on one quarter of the domain only. Therefore it is necessary to incorporate gliding conditions to both symmetry axes. The material parameters are set $E = 206900$, $\nu = 0.29$, $\sigma_Y = 450\sqrt{2/3}$, and $H = 0.5$. Differently to the original example of Stein [46], we choose the modulus of hardening $H$ to be nonzero, i. e., hardening effects are considered. The numerical results concerning the application of the slant Newton method to the the original benchmark problem can be seen in a conference proceedings article of Gruber and Valdman [19].

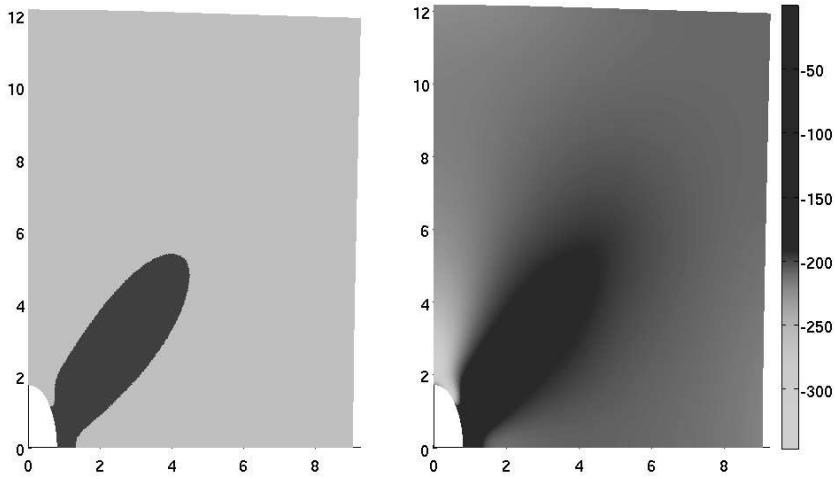


Figure 6: The two plots show plastic zones (left), and the yield function (right) of the deformed domain. For better visibility, the displacement is magnified by a factor 100.

### 1.3.3 Nested iteration strategy for one time step problems

As already mentioned, one important task to speed up the slant Newton method of Section 1.3.2 is to determine good initial values. For a one time step problem, the solution at the present refinement level $l$, can be approximated by the interpolation of the displacement field of the next coarser grid,

$$u_l \approx \mathbb{I}_{l-1}^{l} u_{l-1} .$$

For example, the interpolation operator $\mathbb{I}_{l-1}^{l}$ can be chosen to take the values at coarse grid vertices straight forward, whereas for fine grid vertices, which do not appear in the coarse grid, the initial values are obtained by the mean value of the corresponding neighboring coarse grid vertices. The application of this strategy to the numerical example posed in Figure 5 yields a convergence as displayed in Table 2. The number of iteration steps seems now to be independent of the chosen grid size, which was not so without the nested iteration strategy (cf. Table 1).

| dof: | 245 | 940 | 3680 | 14560 | 57920 | 231040 |
|---|---|---|---|---|---|---|
| dis: | | | | | | |
| 0-1 | 1.669e-02 | 3.036e-02 | 3.649e-02 | 3.908e-02 | 4.006e-02 | 4.035e-02 |
| 1-2 | 3.456e-03 | 4.059e-03 | 5.733e-03 | 6.325e-03 | 6.703e-03 | 6.857e-03 |
| 2-3 | 2.650e-04 | 1.991e-04 | 2.291e-04 | 2.463e-04 | 3.083e-04 | 3.371e-04 |
| 3-4 | 4.976e-08 | 6.206e-08 | 3.661e-06 | 6.981e-06 | 9.366e-06 | 1.022e-05 |
| 4-5 | 5.564e-15 | 1.821e-14 | 1.119e-10 | 1.052e-07 | 6.497e-10 | 3.337e-07 |
| 5-6 | | | 1.848e-15 | 1.115e-13 | 7.246e-15 | 5.351e-08 |
| 6-7 | | | | | | 6.325e-14 |
| res: | | | | | | |
| 0 | 1.637e+03 | 1.184e+03 | 8.466e+02 | 6.019e+02 | 4.268e+02 | 3.022e+02 |
| 1 | 4.182e+01 | 2.504e+01 | 1.730e+01 | 1.647e+01 | 1.789e+01 | 1.317e+01 |
| 2 | 3.463e+00 | 2.405e+00 | 3.088e+00 | 2.184e+00 | 2.003e+00 | 1.661e+00 |
| 3 | 6.948e-04 | 7.978e-04 | 5.445e-02 | 1.007e-01 | 1.265e-01 | 1.374e-01 |
| 4 | 6.925e-11 | 2.341e-10 | 2.033e-06 | 1.458e-03 | 1.029e-05 | 4.622e-03 |
| 5 | 1.163e-11 | 2.402e-11 | 5.433e-11 | 1.475e-09 | 2.204e-10 | 7.041e-04 |
| 6 | | | 5.024e-11 | 1.095e-10 | 2.049e-10 | 1.425e-09 |
| 7 | | | | | | 4.402e-10 |
| sec: | 1 | 4 | 15 | 58 | 234 | 1104 |

Table 1: This table outlines the convergence of the Newton-like method. In horizontal direction, the refinement of the starting mesh takes place, where the degrees of freedom (`dof`) are growing roughly by a factor 4. In the last line (`sec`) the computational time is displayed in seconds. The two blocks in between the first and the last line report on the convergence behavior. The first block (`dis`) displays the distance of two consecutive Newton iterates $|u_{j+1} - u_j|$ measured in the $H^1$ semi norm, the second block (`res`) shows the $l_2$ values of the residual, i. e., the right hand side of Newton's method. The method terminates as the value of `dis` goes below the upper bound $10^{-12}$. Notice, that the last line of the `res`–block shows no more improvement due to rounding errors.

| dof: | 245 | 940 | 3680 | 14560 | 57920 | 231040 |
|---|---|---|---|---|---|---|
| dis: | | | | | | |
| 0-1 | 1.669e-02 | 3.757e-02 | 2.564e-02 | 1.536e-02 | 8.133e-03 | 4.124e-03 |
| 1-2 | 3.456e-03 | 4.981e-03 | 2.559e-03 | 9.493e-04 | 2.478e-04 | 9.472e-05 |
| 2-3 | 2.650e-04 | 1.646e-04 | 5.274e-05 | 3.859e-05 | 8.815e-06 | 2.776e-06 |
| 3-4 | 4.976e-08 | 4.850e-08 | 1.814e-08 | 1.250e-07 | 1.147e-09 | 1.357e-08 |
| 4-5 | 5.581e-15 | 1.160e-14 | 5.741e-15 | 1.337e-13 | 3.872e-15 | 1.388e-14 |
| res: | | | | | | |
| 0 | 1.637e+03 | 8.999e+02 | 7.471e+02 | 5.410e+02 | 3.423e+02 | 1.977e+02 |
| 1 | 4.182e+01 | 8.613e+01 | 2.619e+01 | 1.186e+01 | 3.144e+00 | 1.237e+00 |
| 2 | 3.463e+00 | 2.142e+00 | 5.991e-01 | 3.939e-01 | 1.207e-01 | 3.793e-02 |
| 3 | 6.948e-04 | 6.124e-04 | 2.209e-04 | 1.711e-03 | 1.234e-05 | 1.862e-04 |
| 4 | 6.878e-11 | 1.467e-10 | 7.575e-11 | 1.756e-09 | 1.687e-10 | 3.653e-10 |
| 5 | 1.290e-11 | 2.081e-11 | 4.131e-11 | 8.289e-11 | 1.698e-10 | 3.437e-10 |
| sec: | 1 | 4 | 13 | 53 | 195 | 856 |

Table 2: In this table the same numerical experiment is done as in Table 1 with the nested iteration strategy applied. Notice, that the number of iterations now keeps constant with respect to the degrees of freedom (`dof`).

### 1.3.4 Nested iteration strategy with time evolution

The same strategy also works for time evolving simulations. The time difference of the displacement can be approximated by the interpolation of the same value of the next coarser grid, i. e.,

$$u_l^t - u_l^{t-1} \approx \mathbb{I}_{l-1}^l \left(u_{l-1}^t - u_{l-1}^{t-1}\right) ,$$

where $u_l^t$ is the unknown displacement at the present time step $t$. This leads to the extrapolation rule

$$u_l^t \approx u_l^{t-1} + \mathbb{I}_{l-1}^l \left(u_{l-1}^t - u_{l-1}^{t-1}\right) .$$

In her Master thesis, B. Rauchenschwandtner investigates an application of this nested iteration strategy, which is visualized in Figure 7.

Consider the numerical example as mentioned in Figure 5, but now with a time dependent load $|g| = 450 \sin(t\,\pi)$. Here, $t$ is in $[0, 1.5]$ and the step width regarding the time variable is set to 0.02. The number of Newton iterations at each time step resulting from the nested iteration technique described above is outlined in Table 3.

Further, a good initial value can also be used for predicting the elastoplastic interface, which moves permanently as the loads vary. Due to the non-smoothness of the energy functional at the elastoplastic interface, it is important to resolve this zone with finer mesh size adaptively, whereas higher order ansatz functions and a coarser mesh size can be chosen for the rest of the domain. Therefore, at each time step we consider the mesh to be generated in an spatial adaptive way starting from a fixed coarse mesh which is the same for each time step. One option is to do some uniform refinements before starting the adaptive refinements. This structure leads to different meshes for every time step

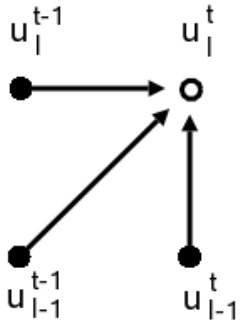


Figure 7: Extrapolation strategy: Previous time step solutions as well as coarse-level solutions are used to create proper initial values for the displacement.

| $t$ | P1 | P2 | $t$ | P1 | P2 | $t$ | P1 | P2 | $t$ | P1 | P2 | $t$ | P1 | P2 |
|---|---|---|---|---|---|---|---|---|---|---|---|---|---|---|
| 0.1 | 2 | 2 | 0.4 | 6 | 6 | 0.7 | 6 | 7 | 1.00 | 2 | 2 | 1.3 | 6 | 6 |
| 0.12 | 2 | 2 | 0.42 | 6 | 6 | 0.72 | 6 | 7 | 1.02 | 2 | 2 | 1.32 | 6 | 6 |
| 0.14 | 5 | 5 | 0.44 | 6 | 6 | 0.74 | 6 | 7 | 1.04 | 2 | 2 | 1.34 | 6 | 6 |
| 0.16 | 5 | 6 | 0.46 | 6 | 6 | 0.76 | 6 | 7 | 1.06 | 2 | 2 | 1.36 | 6 | 6 |
| 0.18 | 5 | 5 | 0.48 | 6 | 6 | 0.78 | 7 | 7 | 1.08 | 2 | 2 | 1.38 | 6 | 6 |
| 0.2 | 6 | 6 | 0.5 | 6 | 7 | 0.8 | 6 | 6 | 1.1 | 2 | 2 | 1.4 | 6 | 6 |
| 0.22 | 7 | 7 | 0.52 | 6 | 6 | 0.82 | 6 | 7 | 1.12 | 2 | 2 | 1.42 | 6 | 6 |
| 0.24 | 6 | 7 | 0.54 | 6 | 6 | 0.84 | 6 | 6 | 1.14 | 5 | 5 | 1.44 | 6 | 6 |
| 0.26 | 6 | 7 | 0.56 | 6 | 6 | 0.86 | 6 | 6 | 1.16 | 5 | 6 | 1.46 | 6 | 6 |
| 0.28 | 6 | 7 | 0.58 | 6 | 7 | 0.88 | 4 | 4 | 1.18 | 5 | 5 | 1.48 | 6 | 6 |
| 0.3 | 6 | 6 | 0.6 | 6 | 6 | 0.9 | 2 | 2 | 1.2 | 6 | 6 | 1.5 | 6 | 7 |
| 0.32 | 6 | 6 | 0.62 | 6 | 7 | 0.92 | 2 | 2 | 1.22 | 7 | 7 | | | |
| 0.34 | 6 | 6 | 0.64 | 6 | 6 | 0.94 | 2 | 2 | 1.24 | 6 | 7 | | | |
| 0.36 | 6 | 6 | 0.66 | 6 | 6 | 0.96 | 2 | 2 | 1.26 | 6 | 7 | | | |
| 0.38 | 6 | 6 | 0.68 | 6 | 6 | 0.98 | 2 | 2 | 1.28 | 6 | 7 | | | |

Table 3: Number of Newton steps for the problem posed in Figure 5 with a time dependent load, $|g| = 450 \sin(t\,\pi)$, at a uniform refinement level 4 (P1, degrees of freedom: 14560), and at an adaptive refinement level 6 (P2, degrees of freedom vary from 24000 to 32000).

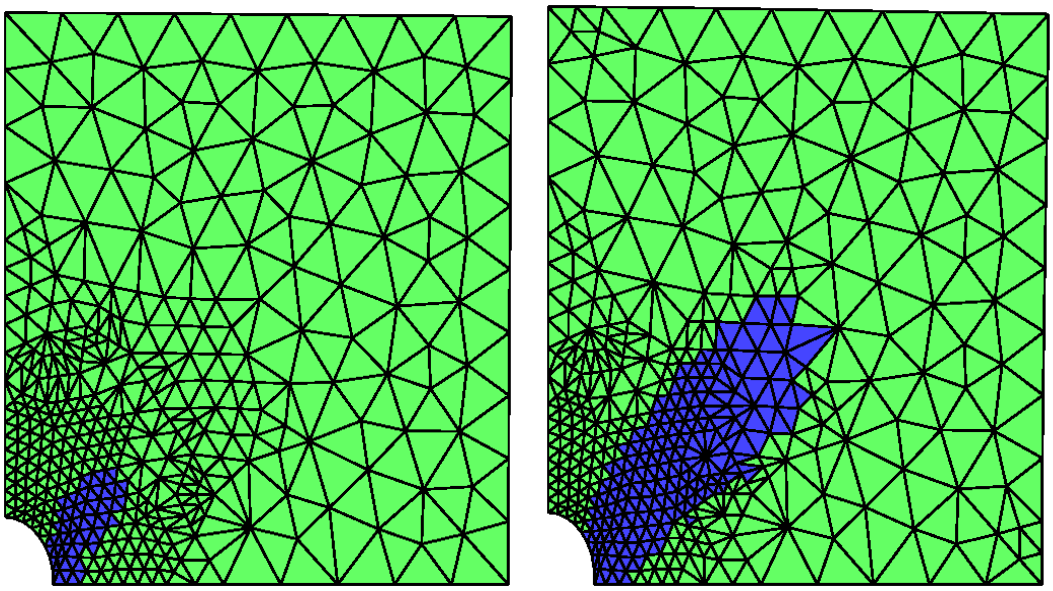

Figure 8: Two different adaptive meshes, both at adaptive refinement level 3 but subject to different loads. The plastic domain is colored blue (dark in gray scale), whereas the elastic domain is colored green (light in gray scale). Notice, that each of the two meshes consists of vertices, which do not appear in the other mesh.

(incremental step) in which the solution is calculated. As it is shown in Figure 8, the meshes of the same refinement level can be quite different at two different time steps, i. e. in general there exists no common vertex except for the vertices of the coarsest mesh (refinement level 0). Thus, one has to define another interpolation operator between the meshes of two different time steps, $\mathbb{I}_{t-1}^{t}$, and ends up with a slightly modified extrapolation formula

$$u_l^t \approx \mathbb{I}_{t-1}^{t}\, u_l^{t-1} + \mathbb{I}_{l-1}^{l}\, \left(u_{l-1}^{t} - \mathbb{I}_{t-1}^{t}\, u_{l-1}^{t-1}\right) .$$

Notice, that due to the nested iteration technique, not only the solution on the finest mesh per time step is calculated, but rather a series of solutions on each refinement level in every time step. Table 3 reports on the number of Newton steps needed for the finest (adaptive) level. Other numerical examples dealing with nested iteration strategies and interface prediction can be found in B. Rauchenschwandtner [40].

It is shown, that by using this nested iteration technique, and by assuming higher regularity of the solution, e. g. $u(t) \in H^2(\Omega)$ for all $t$, the number of Newton iterations does neither depend on the number of refinement levels nor on the step width regarding the time variable.

### 1.3.5 Modeling of multi yield elastoplasticity

J. Valdman together with M. Brokate and C. Carstensen published his results on analysis, see Brokate, Carstensen and Valdman [5] and numerical treatment, see Brokate, Carstensen and Valdman [7] of multi-yield plasticity models. The main feature of the multi-yield models is higher number of plastic strains $p_1, \ldots, p_N$ used for more realistic modeling of the elasto-plastic transition. It was possible to prove the existence and uniqueness of the corresponding variational inequalities and design a FEM based solution algorithm. Since the structure of the minimization functional in the multi-yield plasticity model remains the same as for the single-yield model discussed above, a direct modification of an existing elastoplasticity package [29] as a part of the Netgen/NGSolve software was feasible [33]. In addition to older Matlab examples, a new 3D calculation performed in Netgen/NGSolve was added [7]. Figure 9 displays (blue) elastic, (red) first and (green) second plastic deformational zones of the shaft model.

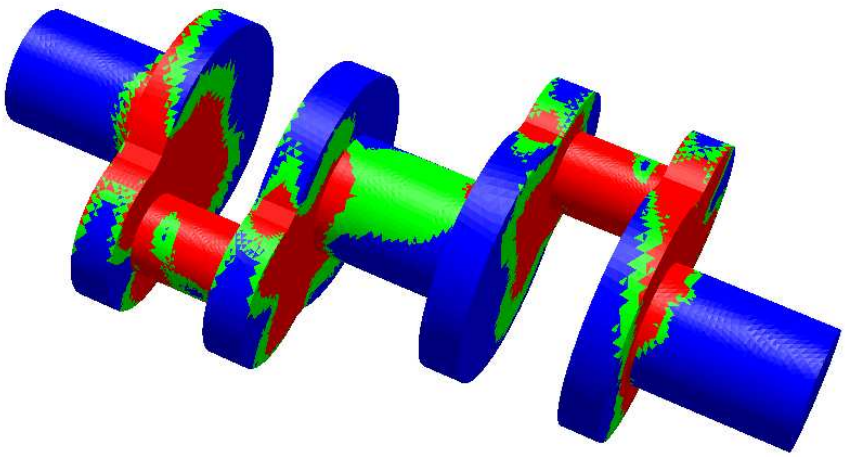

Figure 9: Example of a two-yield plasticity distribution.

A. Hofinger from Project F1308 and J. Valdman also concentrated on fast calculation techniques for the two-yield elastoplastic problem, which is a locally defined, convex but non-smooth minimization problem for the unknown plastic-strain increment matrices $p_1$ and $p_2$. So far, the only applied technique was an alternating minimization, whose convergence is known to be geometrical and global. They showed that symmetries can be utilized to obtain a more efficient implementation of the alternating minimization. For the first plastic time-step problem, which describes the initial elastoplastic transition, the exact solution for $p_1$ and $p_2$ could even be obtained analytically. In the later time-steps used for the computation of the further development of elastoplastic zones in a

continuum, an extrapolation technique as well as a Newton-algorithm were proposed. Their results were summarized in a technical report [24] and were also accepted for a journal publication, see Hofinger and Valdman [25]. Alternatively, some symbolic techniques were applied in order to study a system of two polynomial for the unknowns $\xi_1 = ||p_1||$ and $\xi_2 = ||p_1||$ in case that both $||p_1||$ and $||p_1||$ are positive (this correspond to the activation of both plastic zones). Together with B. Buchberger and W. Windsteiger from Project F1302 we managed to calculate the Gröbner base which gives insight to the structure of solutions of the simultaneous system. It has also been confirmed that no explicit formula can be found and the local minimization problem needs to be solved approximatively for general material parameters and deformation states. In cooperation with Project F1303 a combined numerical-symbolic method based on the Synaps package was tested. One example of polynomial systems was also used for testing of a geometry based solver by B. Jüttler (from Project 1315) and Bartoň [2].

### 1.3.6 *h*-adaptivity for nonlinear (elastoplastic) problems

In cooperation with C. Carstensen and A. Orlando (both HU Berlin), an adaptive finite element algorithm for the solution of elastoplastic problems Carstensen, Orlando and Valdman [12] has been established. Such an algorithm yields an energy reduction and, up to higher order terms, the $R-$linear convergence of the stresses with respect to the number of loops. Applications include several plasticity models: linear isotropic-kinematic hardening, linear kinematic hardening, and multi-surface plasticity as a model for nonlinear hardening laws. Numerical examples confirm an improved linear convergence rate, the performance of the algorithm in comparison with the more frequently applied maximum refinement rule is studied in Figure 10.

J. Valdman also cooperated also with S. Repin (St. Petersburg) on reliable error estimates for the scalar nonlinear problem, where the nonlinearity is defined on a part of the boundary. Such system can be easily described as a variational inequality. They derived a-posteriori estimates of the difference between the exact solution of such type variational inequalities and any function lying in the admissible functional class of the problem considered. It is shown that the structure of the error majorant reflects properties of the exact solution. The majorants provide guaranteed upper bounds of the error for any conforming approximation and possess necessary continuity properties. In the series of numerical tests performed, it was shown that the estimates are explicitly computable, they provide sharp bounds of approximation errors, and they give high quality indication of the distribution of local (element-wise) errors. Their research was documented in a joint paper Repin and Valdman [41] and will be extended for elastic problems with so-called friction boundary conditions and later to elastoplasticity as well Repin and Valdman [42].

Another issue being studied is the computational efficiency of "functional estimates"

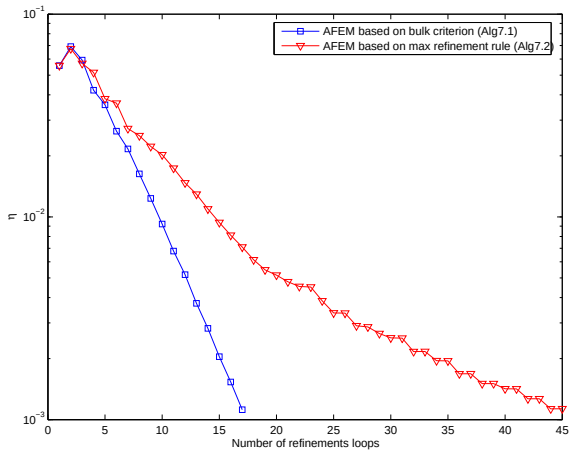


Figure 10: Comparison of the new adaptive algorithm (blue line) and the original algorithm based on the maximum refinement rule (red line). Note that using the new algorithm, the energy of the elastoplastic solution is linearly reduced with each refinement step.

even in the linear case. Let us consider the boundary value problem

$$-\triangle u = f \quad \text{in } \Omega, \quad u = 0 \quad \text{on } \partial\Omega.$$

Then, one can find a norm estimate of the form

$$||\nabla(u - v)||_0 \leq ||\nabla v - y^*||_0 + C_\Omega ||\text{div} y^* + f||_0$$

which is valid for all $y^* \in H(\Omega, \text{div})$ and for all $v \in H_0^1$. The constant $C_\Omega$ is known from Friedrich's inequality and can be computed independently. The interpretation of this formula is that any "flux" function $y^*$ provides us with a guaranteed upper bound

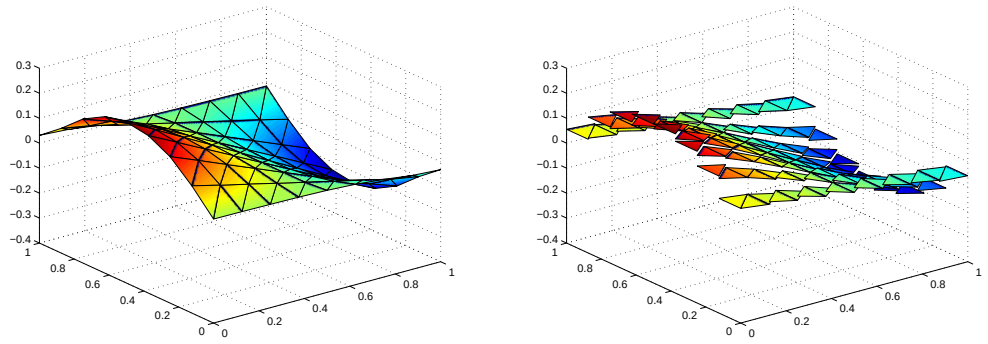

Figure 11: Flux function (x-component) using nodal *(left)* and Raviart-Thomas *(right)* elements.

for the energy error of the computed solution $v$. The right term in the inequality can be minimized in a way, the upper bound becomes the smallest possible. The pictures presented in Figure 11 demonstrate possible "fluxes" using nodal continuous and normal component continuous (Raviart-Thomas) elements. Such minimization leads to a linear system of equations as a part of the global nonlinear minimization process. J. Valdman explored these linear systems and applied a multigrid based solver in order to obtain the optimal convergence.

## 1.4 Collaboration Within and Outside the SFB

### 1.4.1 Internal Cooperations

*There were cooperations with the following subprojects:*

- **Subproject F1301**: Another basic research topic for *hp*-FEM has been the development of a basis in which the element stiffness matrix is sparse. The sparsity is known for tensor product elements like the square or cube using integrated Legendre polynomials, see [47], but not for triangular and tetrahedral elements. In our paper [4], we have defined a basis on the reference triangle in which the element stiffness matrix has $\mathcal{O}(p^2)$ nonzero entries. The definition of the basis functions uses Jacobi polynomials. Moreover, explicit formulas for the remaining nonzero entries are given. Using this result, the global stiffness matrix can be computed in $\mathcal{O}(p^2)$ flops if

  - all elements are triangles and
  - a convection-reaction-diffusion equation with piecewise constant or piecewise polynomial coefficients is considered.

  Moreover, the matrix vector multiplication can be performed in optimal arithmetical complexity.

  The results have been extended to the reference tetrahedron in the paper [3] with V. Pillwein from project F1301. The proof of the sparsity of the element stiffness matrix, which is the central theorem of this paper, has been done for several families of basis functions with a Mathematica program, see project F1301. In a proceedings paper with V. Pillwein, another basis functions have been investigated in which the proof in [3] has been necessary to modify.

- **Subproject F1308**: *A. Hofinger brought some new ideas to the solution of multi-yield minimization problems which are described in a joint publication* Hofinger and Valdman *[25].*

- **Subproject F1309**: *This cooperation is naturally strong and includes the numerical analysis as well as the implementation of finite element software including*

*geometry and mesh handling. Apart from this J. Valdman was advised by R. Simon on an implementation of a multigrid solver appearing in functional a-posteriori estimates.*

- **Subproject F1315**: *A new system for solving system of polynomials* Jüttler and Bartoň *[2] uses a polynomial system from* Hofinger and Valdman *[25] as one of its benchmarks. A new system for solving system of polynomials* Jüttler and Bartoň *[2] uses a polynomial system from* Hofinger and Valdman *[25] as one of its benchmarks.*

### 1.4.2 External Cooperations

- April 1 - July 31, 2007: P. G. Gruber investigated the solution of elastoplastic problems based on mixed variational formulations together with J. Schöberl at the Department for Mathematics CCES (Center for Computational Engineering Science), RWTH Aachen.

*The following cooperations have led to joint publications:*

- *Prof. C. Carstensen (Technical University Vienna, Austria) and Prof. M. Brokate (Technical University Munich, Germany): Multi-yield plasticity, see* Brokate, Carstensen, and Valdman *[5, 7]; A posteriori error estimates, see* Carstensen, Orlando and Valdman *[12].*
- *Prof. S. Repin (Steklov Institute of Mathematics, St. Petersburg, Russia: functional aposteriori error estimates* Repin and Valdman *[43].*

## References

[1] J. Alberty, C. Carstensen, and D. Zarrabi. Adaptive numerical analysis in primal elastoplasticity with hardening. *Comput. Methods Appl. Mech. Eng.*, 171(3-4):175–204, 1999.

[2] M. Bartoň and B. Jüttler. Computing roots of systems of polynomials by linear clipping. *Mathematics of Computation.* (submited).

[3] S. Beuchler and V. Pillwein. Sparse shape functions for tetrahedral $p$-fem using integrated jacobi polynomails using integrated jacobi polynomials. *Computing*, 2007. to appear.

[4] S. Beuchler and J. Schöberl. New shape functions for triangular p-fem using integrated jacobi polynomials. *Num. Math.*, 2005. (submitted).

[5] M. Brokate, C. Carstensen, and J. Valdman. A quasi-static boundary value problem in multi-surface elastoplasticity: Part 1 – analysis. *Math. Meth. Appl. Sciences*, 27(14):1697–1710, 2004.

[6] M. Brokate, C. Carstensen, and J. Valdman. A quasi-static boundary value problem in multi-surface elastoplasticity: Part 1 – numerical solution. SFB Report 2004-11, Johannes Kepler University Linz, SFB F013 "Numerical and Symbolic Scientific Computing", 2004.

[7] M. Brokate, C. Carstensen, and J. Valdman. A quasi-static boundary value problem in multi-surface elastoplasticity: Part 2 – numerical solution. *Math. Meth. Appl. Sciences*, 28(8):881–901, 2005.

[8] M. Brokate, C. Carstensen, and J. Valdman. A quasi-static boundary value problem in multi-surface elastoplasticity: Part 1 – analysis. SFB Report 2003-16, Johannes Kepler University Linz, SFB F013 "Numerical and Symbolic Scientific Computing", 2006.

[9] C. Carstensen. Domain decomposition for a nonsmooth convex minimization problem and its application to plasticity. *NLAA*, 4(3):1–13, 1997.

[10] C. Carstensen, A. Orlando, and J. Valdman. A convergent adaptive finite element method for the primal problem of elastoplasticity. Technical Report 2005-12, Institute of Mathematics, Humboldt-Universitaet zu Berlin, 2005.

[11] C. Carstensen, A. Orlando, and J. Valdman. A convergent adaptive finite element method for the primal problem of elastoplasticity. *Inter. J. Numer. Meth. Engns.*, 67(13):1851–1887, 2007.

[12] C. Carstensen, V. Orlando, and J. Valdman. A convergent adaptive finite element method for the primal problem of elastoplasticity. *International Journal for Numerical Methods in Engineering*, 67(13):1851–1887, 2006.

[13] X. Chen, Z. Nashed, and L. Qi. Smoothing methods and semismooth methods for nondifferentiable operator equations. *SIAM Journal on Numerical Analysis*, 38(4):1200–1216, 2000.

[14] A. Düster. *High order finite elements for three-dimensional, thin walled nonlinear continua*. PhD thesis, Technical University Munich, 2001. Shaker publishing, 2002.

[15] G. Duvaut and J.L.Lions. *Inequalities in Mechanics and Physics*. Springer, Berlin Heidelberg New-York, 1976.

[16] K. Eriksson, D. Estep, P. Hansbo, and C. Johnson. Introduction to adaptive methods for differential equations. *Acta Numerica*, pages 105–158, 1995.

[17] P. Gruber and J. Valdman. New numerical solver for elastoplastic problems based on the Moreau-Yosida theorem. SFB Report 2006-05, Johannes Kepler University Linz, SFB "Numerical and Symbolic Scientific Computing", 2006.

[18] P. G. Gruber. Solution of elastoplastic problems based on the Moreau-Yosida theorem. Master's thesis, Johannes Kepler University Linz, 2006.

[19] P. G. Gruber and J. Valdman. Implementation of an elastoplastic solver based on the Moreau-Yosida Theorem. *Elsevier, Math. Comput. Simul.*

[20] P. G. Gruber and J. Valdman. Newton-like solver for elastoplastic problems with hardening and its local super-linear convergence. SFB Report 6, Johannes Kepler University Linz, SFB F013 "Numerical and Symbolic Scientific Computing", 2007.

[21] W. Han and B. Reddy. Computational plasticity: The variational basis and numerical analysis. *Computer methods in applied mechanics and engineering*, pages 283–400, 1995.

[22] W. Han and B. D. Reddy. *Computational Plasticity: Mathematical theory and numerical analysis*. Springer, Berlin, Heidelberg, New York, 1999.

[23] I. Hlaváček, J. Haslinger, J. Nečas, and J. Lovíšek. *Solutions of Variational Inequalities in Mechanics*. Springer-Verlag New York, 1988.

[24] A. Hofinger and J. Valdman. Numerical solution of the two-yield elastoplastic minimization problem. Technical report, Johannes Kepler University Linz, SFB F013 "Numerical and Symbolic Scientific Computing", 2006.

[25] A. Hofinger and J. Valdman. Numerical solution of the two-yield elastoplastic minimization problem. *Computing*, 2007. (accepted).

[26] J.C.Simo and T. Hughes. *Computational Inelasticity*. Springer, 1998.

[27] C. Johnson. Existence theorems for plasticity problems. *J. math. pures et appl.*, 55:431–444, 1976.

[28] J. Kienesberger. Multigrid preconditioned solvers for some elasto-plastic problems. SFB Report 03-15, Johannes Kepler University Linz, SFB "Numerical and Symbolic Scientific Computing", 2003.

[29] J. Kienesberger. Multigrid preconditioned solvers for some elastoplastic problems. In I. Lirkov, S. Margenov, J. Waśniewski, and Y. P., editors, *Proceedings of LSSC 2003*, volume 2907 of *Lecture Notes in Computer Science*, pages 379–386. Springer, 2004.

[30] J. Kienesberger. *Efficient Solution Algorithms for Elastoplastic Problems*. PhD thesis, Johannes Kepler University Linz, 2006.

[31] J. Kienesberger, U. Langer, and J. Valdman. On a robust multigrid-preconditioned solver for incremental plasticity problems. In *Proceedings of IMET 2004 - Iterative Methods, Preconditioning & Numerical PDEs*, pages 84–87, 2004.

[32] J. Kienesberger and J. Valdman. An efficient solution algorithm for elastoplasticity and its first implementation towards uniform h- and p- mesh refinements. In *Proceedings of ENUMATH 2005*.

[33] J. Kienesberger and J. Valdman. Multi-surface elastoplastic continuum - modelling and computations. In M. Feistauer, V. Dolejsi, P. Knobloch, and K. Najzar, editors, *Numerical Mathematics and Advanced Applications*, pages 539–548. Springer, 2004. Proceedings of ENUMATH 2003.

[34] V. G. Korneev and U. Langer. *Approximate solution of plastic flow theory problems*, volume 69 of *Teubner-Texte zur Mathematik [Teubner Texts in Mathematics]*. BSB B. G. Teubner Verlagsgesellschaft, Leipzig, 1984. With German, French and Russian summaries.

[35] J. Moreau. Proximité et dualité dans un espace hilbertien. *Bulletin de la Société Mathématique de France*, 93:273–299, 1965.

[36] Netgen. Download of netgen: http://www.hpfem.jku.at/netgen/index.html.

[37] NGSolve. Download of ngsolve: http://www.hpfem.jku.at/ngsolve/index.html.

[38] V. Nübel. *Die adaptive rp-Methode für elastoplastische Probleme*. PhD thesis, Technical University Munich, 2005. Shaker publishing, 2006.

[39] V. Nübel, A. Düster, and E. Rank. An rp-adaptive finite element method for elastoplastic problems. Accepted for publication in Computational Mechanics, 2006.

[40] B. Rauchenschwandnter. Nested iteration strategies for 2d elasto-plastic problems. Master's thesis, Johannes Kepler University Linz, 2007.

[41] J. Repin and V. J. Functional a posteriori error estimates for problems with nonlinear boundary conditions. *Journal of Numerical Mathematics*, 2007. (accepted).

[42] S. Repin and J. Valdman. Functional a posteriori error estimates for elastoplastic problems. Technical report. (in preparation).

[43] S. Repin and J. Valdman. Functional a posteriori error estimates for problems with nonlinear boundary conditions. Technical Report 2006-25-18, Johannes Kepler University Linz, Johannes Radon Institute for computational and applied mathematics (RICAM), 2006.

[44] J. Schöberl. Netgen: An advancing front 2d/3d-mesh generator based on abstract rule. *Computing and Visualization in Science*, 1(1):41–52, 1997.

[45] H. Schwarz. *Methode der finiten Elemente. Eine Einführung unter besonderer Berücksichtigung der Rechenpraxis*, volume 47 of *Teubner Studienbücher Mathematik; Leitfäden der Angewandten Mathematik und Mechanik*. Teubner, 3rd edition, 1991.

[46] E. Stein, editor. *Error-Controlled Adaptive Finite Elements in Solid Mechanics*. John Wiley & Sons Ltd., 2003.

[47] B. A. Szabo and I. Babuska. *Finite Element Analysis*. Wiley, 1991.